Anti-aging effects of vitamin C on human pluripotent stem cell-derived cardiomyocytes

Yoon Young Kim · Seung-Yup Ku · Yul Huh ·
Hung-Ching Liu · Seok Hyun Kim ·
Young Min Choi · Shin Yong Moon

Abstract Human pluripotent stem cells (hPSCs) have arisen as a source of cells for biomedical research due to their developmental potential. Stem cells possess the promise of providing clinicians with novel treatments for disease as well as allowing researchers to generate human-specific cellular metabolism models. Aging is a natural process of living organisms, yet aging in human heart cells is difficult to study due to the ethical considerations regarding human experimentation as well as a current lack of alternative experimental models. hPSC-derived cardiomyocytes (CMs) bear a resemblance to human cardiac cells and thus hPSC-derived CMs are considered to be a viable alternative model to study human heart cell aging. In this study, we used hPSC-derived CMs as an in vitro aging model. We generated cardiomyocytes from hPSCs and demonstrated the process of aging in both human embryonic stem cell (hESC)- and induced pluripotent stem cell (hiPSC)-derived CMs. Aging in hESC-derived CMs correlated with reduced membrane potential in mitochondria, the accumulation of lipofuscin, a slower beating pattern, and the downregulation of human telomerase RNA (hTR) and cell cycle regulating genes. Interestingly, the expression of hTR in hiPSC-derived CMs was not significantly downregulated, unlike in hESC-derived CMs. In order to delay aging, vitamin C was added to the cultured CMs. When cells were treated with 100 μM of vitamin C for 48 h, anti-aging effects, specifically on the expression of telomere-related genes and their functionality in aging cells, were observed. Taken together, these results suggest that hPSC-derived CMs can be used as a unique human cardiomyocyte aging model in vitro and that vitamin C shows anti-aging effects in this model.

Keywords Aging · Cardiomyocyte · Human pluripotent stem cell · Vitamin C

Y. Y. Kim · S.-Y. Ku · Y. Huh · S. H. Kim · Y. M. Choi ·
S. Y. Moon
Institute of Reproductive Medicine and Population,
Medical Research Center, Seoul National University,
Seoul, South Korea

S.-Y. Ku (✉) · S. H. Kim · Y. M. Choi · S. Y. Moon
Department of Obstetrics and Gynecology,
College of Medicine, Seoul National University,
Seoul 110-744, South Korea
e-mail: jyhsyk@snu.ac.kr

H.-C. Liu
Center for Reproductive Medicine and Infertility,
Weill Cornell Medical College,
New York, NY 10021, USA

Introduction

Human pluripotent stem cells (hPSCs), including human embryonic stem cells (hESCs) (Thomson

et al. 1998; Oh et al. 2005a) and human induced pluripotent stem cells (hiPSCs) (Takahashi et al. 2007), possess the ability to differentiate into any of the cells of the body including cardiomyocytes (CMs) (Kehat et al. 2001; Mummery et al. 2003; Kim et al. 2008; Yokoo et al. 2009). hESCs are derived from the inner cell mass of blastocyst (Thomson et al. 1998) and hiPSCs are stem cells derived from adult somatic cells that have been reprogrammed to an embryonic-like state (Takahashi et al. 2007). Regardless of their origins, whether from hESCs or hiPSCs, hPSC-derived CMs are expected to serve as an unlimited source of cells for cell-based therapy of cardiac disease and an alternative cellular model of human cells for cardiovascular drug screening, heart developmental studies, and human aging experiments (Kim et al. 2011).

Human cardiomyocytes are the main structural cells of the heart. These cells are essential for the contraction of heart, a functionality that is lost in cardiac disease such as myocardial infarction (Laflamme and Murry 2005) as well as during aging process (Terman and Brunk 1998). To investigate the effect of aging on cardiomyocytes, age-related alterations must be observed and the affecting factors must be discovered. Little is known about the aging of cardiac cells and their age-related alterations (Terman et al. 2003) due to the fact that live cardiomyocytes cannot be easily obtained from the human body for studies in vitro. Therefore, the development of hPSC-derived CMs may serve as an important model for human-originated cardiomyocytes studies in the laboratory.

In this study, we observed the aging phenomena in hPSC-derived cardiac cells generated by our previously reported method (Kim et al. 2011) and described the characteristics of naturally aged, hPSC-derived cardiac cells. The aged cardiac cells showed a weaker and slower beating pattern as well as increased expression of senescence-associated (SA) β-galactosidase. Additionally, decreased expression of the aging-related genes hTR and TRF2 and cell cycle regulating genes including cyclin D1, cyclin D2, cyclin D3, and Cdk2 and an accumulation of aging pigment lipofuscin were observed. Exposure to 100 μM of vitamin C for 48 h reversed the effects of aging in hESC-derived CMs.

Materials and methods

Human pluripotent stem cell culture and differentiation into cardiomyocytes

The SNUhES3, human ESC line, was purchased from Seoul National University (Oh et al. 2005a) and hiPSCs from System Biosciences (SBI, Mountain View, CA, USA). Human PSCs were maintained as previously described (Oh et al. 2005b). Undifferentiated hPSCs were replated onto mitotically inactivated feeder layer cells (STO, CRL-1503, ATCC, Manassas, VA, USA) every 7 days. DMEM/F12 (Invitrogen, Calsbad, CA, USA) supplemented with 20 % knockout serum replacement (KO-SR; Invitrogen), 1 % MEM NEAA (Invitrogen), 0.1 mM β-mercaptoethanol (Sigma, St. Louis, MO, USA), 50 U/ml penicillin (Invitrogen), 50 ug/ml streptomycin (Invitrogen), and 4 ng/ml basic fibroblast growth factor (bFGF; Invitrogen) was used as the culture medium for hPSCs.

To induce differentiation into cardiomyocyte, 5–7-day-old hPSCs were treated with 0.25 % trypsin-EDTA (Invitrogen) for 5 min. The detached feeder cells were then removed, and the hPSCs were washed with phosphate-buffered saline (PBS). Then, 100 ng/ml of activin A (R&D Systems, Minneapolis, MN, USA) and 10 ng/ml of BMP2 (R&D Systems) were added for 5 days. The differentiation medium consisted of RPMI 1640 (Invitrogen) supplemented with B27 (Invitrogen) (Kim et al. 2011).

To replate differentiated cells, 1 ml of TrypLE express (Invitrogen) was treated and incubated for 5 min at 37 °C. Dissociated cells were washed and resuspended with RPMI 1640 (Invitrogen) supplemented with B27 (Invitrogen) and plated.

Treatment of vitamin C

The experimental concentrations of L-ascorbic acid (Sigma) were 0, 100, and 250 μM and treated for 24 h at days 11, 17, and 23. For the 48 h treatment, L-ascorbic acid was added to cells on days 10–12, 16–18, and 22–24.

Immunolabeling

To evaluate the localization of specific proteins, cells were washed with PBS (Sigma) and fixed with 4 %

paraformaldehyde (PFA; Sigma) for 15 min at room temperature (RT). To inhibit non-specific binding, 3 % bovine serum albumin (Sigma) solution was added and the cells were then incubated for 1 h at RT. Primary antibodies (1:100) included mouse anti-Nkx2.5 (R&D Systems), rabbit anti-Nkx2.5 (Abcam, Cambridge, MA, USA), goat anti-α-myosin heavy chain (anti-αMHC; SantaCruz Biotechnology, Santa-Cruz, CA, USA), rabbit anti-atrial natriuretic factor

(anti-ANF; SantaCruz Biotechnology), and mouse troponin I (anti-cTn I: Chemicon, Billerica, MA, USA). They were applied for 1 h at RT. The cells were then washed with PBS with Triton X100 (PBST; Sigma) three times. The secondary antibodies, which included Alexa Fluor 488-labeled donkey anti-mouse and rabbit IgG, Alexa Fluor 594-labeled donkey anti-mouse, and goat and rabbit IgG (Molecular Probes, Calsbad, CA, USA), were applied for 1 h at RT in the dark and
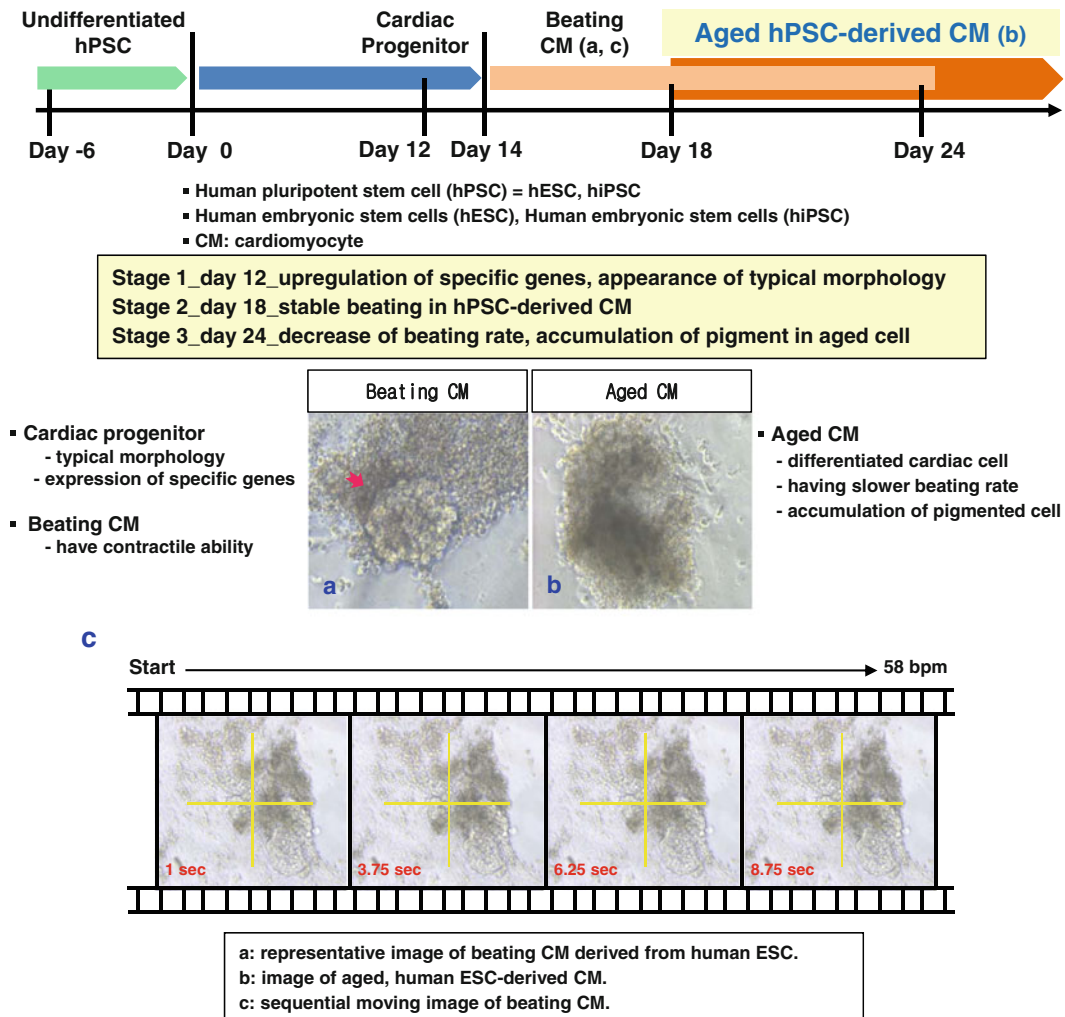

Fig. 1 Schematic representation of experiments. The definition and features of CMs derived from hPSCs, which include hESCs and hiPSCs, are indicated for each temporal stage. Representative pictures of beating and aged CMs are included for illustration. a A representative image of beating CMs. The contractile region is indicated by the *red arrow*. b The morphology of aged CMs. As the in vitro culture period lengthened, the differentiated cells showed a *darker color* in the center region and the beating rate decreased. c Sequential moving images of beating CMs are temporally arranged from *left* to *right*, and the time is indicated at the *bottom-left* of each image in *red*

washed with PBST three times. Cells were treated with Prolong gold anti-fade reagent with DAPI (Invitrogen) and analyzed using laser scanning microscopy (BioRad, Carlsbad, CA, USA).

Quantitative RT-PCR

Total RNA was extracted from cells using Trizol (Invitrogen) according to the manufacturer's instructions. cDNA was synthesized from 1 μg of RNA using the Accute RT Premix (Bioneer, Daejeon, Korea). Quantitative PCR was carried out with the RotorGene 3000 (Corbett Life Science, Valencia, CA, USA) using the QuantiTect™ SYBR® Green PCR kit (Qiagen, Valencia, CA, USA). The amplification program comprised of an initial step at 95 °C for 15 min, followed by 45 cycles of denaturation at 95 °C for 15 s per cycle, an annealing step at 58 °C for 20 s, and then a final extension step at 72 °C for 30 s. All reactions were run in triplicate. C_T was calculated under default settings of RotorGene 6.0 software (Corbett Life Science). Gene expression was normalized to GAPDH expression.

FACS analysis

Samples were dissociated into single cells using 0.25 % trypsin-EDTA. Dissociated cells were fixed with 4 % PFA for 15 min at RT. The cells were then washed with PBS by centrifugation at 1,500 rpm for 5 min. Primary antibodies, mouse anti-Nkx2.5 and goat anti-αMHC, were applied for 1 h at RT. The cells were subsequently washed with PBS by centrifugation twice. Secondary antibodies, Alexa Fluor 488-labeled donkey anti-mouse and Alexa Fluor 594-labeled donkey anti-goat IgG, were applied for 1 h at RT in the dark and washed with PBS by centrifugation twice. The samples were analyzed using FACS Calibur™ and FACS Aria-I (BD Biosciences, San Diego, CA, USA).

Senescence-associated beta-galactosidase staining

The medium was removed from the samples and washed with PBS carefully. Then, 1× fixing solution was added and incubated for 10 min at RT. Following rinsing with PBS twice, 1× staining solution containing X-Gal (Intron Biotechnology, Seoul, Korea) was added to samples and incubated overnight at 37 °C. After incubation, the staining solution was removed

and the cells were washed with PBS twice. Samples were analyzed under a light microscope (Nikon, Tokyo, Japan).

Transmission electron microscopy

The samples were washed with PBS and fixed with 2.5 % glutaraldehyde (Sigma) for 20 min at RT. The cells were then fixed with 1 % osmium tetroxide (Sigma) supplemented with 0.14 M sucrose (Sigma) for 10 min at 4 °C. Cells infiltrated with epoxy resin were transferred to beam capsules for polymerization. Ultra-thin sections were obtained using an ultramicrotome (MT-6000; DuPont Instruments-Sorvall Biomedical Div., Wilmington, DE, USA), and samples were observed under transmission electron microscope (JEM-1400; JEOL Ltd., Tokyo, Japan).

TRAP assay

Samples for the TRAP assay were prepared using the TRAPeze® Telomerase Detection Kit (Millipore, Billerica, MA, USA), according to the manufacturer's instructions. Briefly, each stage of cells was lysed using lysis buffer and centrifugated for 20 min at 4 °C. The collected supernatant was used as a template for PCR amplification. The PCR amplification program consisted of denaturation at 94 °C for 30 s,

Fig. 2 Evaluation of cardiac characteristics in hPSC-derived CMs. The expression of cardiac-specific genes was evaluated at the mRNA and protein level. Each stage of differentiation in hPSCs demonstrated expression of critical cardiac cascade genes. **A** Immunostaining of hPSC-derived CMs. Expression of cardiac specific genes in hESC-derived (*a–e*) and hiPSC-derived CMs (*f–j*) at each stage. Cardiac transcription factor Nkx2.5, protein for contraction cardiac troponin I (cTnI), structural protein αMHC, and the cardiomyocyte secreting protein ANF were immunolabeled and evaluated using laser scanning microscopy. Images were captured at 200× magnification (*insets*) and enlarged images at 800× magnification are represented. *a, f* Stage 1(day 12), Nkx2.5 (*green*), cTn I (*red*); *b, g* stage 2 (day 18), Nkx2.5 (*green*), αMHC (*red*); *d, i* stage 3 (day 24), Nkx2.5 (*green*), ANF (*red*). Images of replated hESC-derived (*c, e*) and hiPSC-derived CMs (*h, j*) were captured at 200× magnification (*insets*) and enlarged images at 1,200× magnification are represented. *c, h* Stage 2 (day 18), Nkx2.5 (*green*), αMHC (*red*); *e, j* stage 3 (day 24), Nkx2.5 (*green*), ANF (*red*). **B** Expression of cardiac specific genes in hPSC-derived CMs using qRT-PCR. Expression level was normalized to GAPDH and run in triplicate. **C** Positive populations for Nkx2.5 and αMHC were evaluated. More than 60 % of differentiated cells were positive for Nkx2.5 and αMHC as measured by FACS analysis
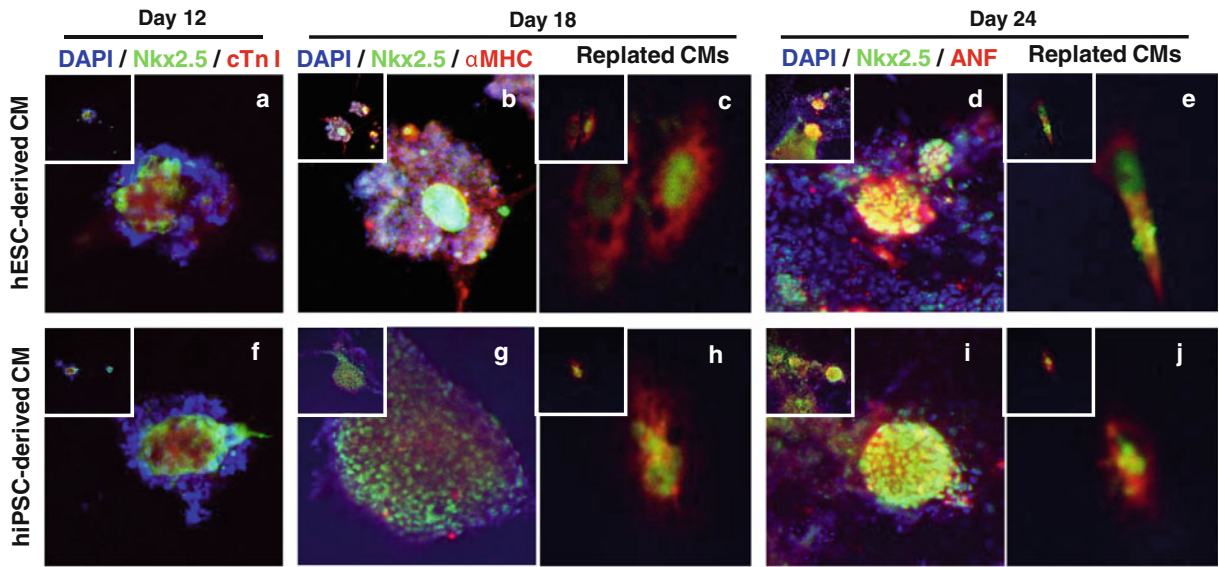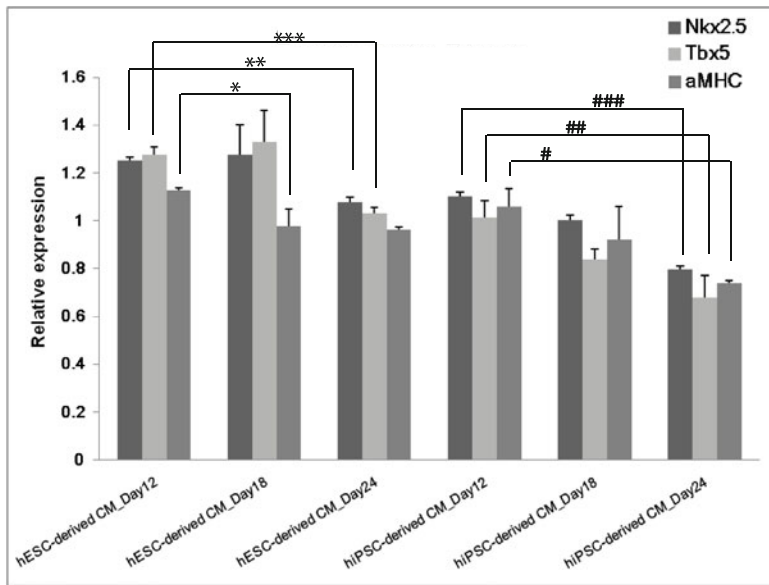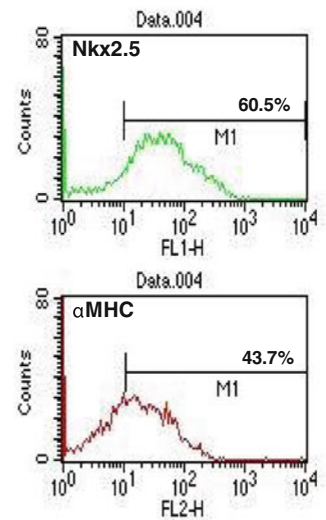
annealing at 59 °C for 60 s, and extension at 72 °C for 60 s, for 60 cycles. PCR products were run in non-denaturing PAGE and visualized using SYBR green I (Sigma) staining.

JC-1 staining

Freshly prepared media were added to samples, and 10 µg/ml of JC-1 (Invitrogen) solution was added. An

incubation for 10 min at 4 °C followed, and the cells were then washed with culture media. Fluorescence of labeled cells was observed using fluorescence microscopy (Nikon, Tokyo, Japan) and confocal laser scanning microscopy. In preparation for fluorescence analysis, JC-1 stained cells were dissociated with 0.25 % trypsin-EDTA. Dissociated cells were resuspended in PBS and analyzed using FACS Calibur[TM] (BD Biosciences).

Statistical analysis

Data were analyzed with one-way ANOVA, and post-hoc comparison of means was conducted by Duncan's test. All experiments were performed in triplicate. Significance was accepted for p value less than 0.05 ($p < 0.05$). Calculations were conducted with the Statistical Package for the Social Sciences for Windows (version 12.0, SPSS Inc., Chicago, IL, USA).

Results

hPSC differentiation into cardiomyocytes

hESCs and hiPSCs differentiation was induced using our previously described method (Kim et al. 2011). The experimental scheme is represented in Fig. 1. We classified differentiated cells into three stages according to their in vitro culture period: day 12 (stage 1), day 18 (stage 2), and day 24 (stage 3). Images of functional, hESC-derived CM (Fig. 1a) and aged CM (Fig. 1b) showed the typical morphology of differentiated CMs and their age-related alterations. Functional cardiomyocytes showed regular beating in vitro and real-time sequential images of beating were acquired (Fig. 1c).

Characterization of hPSC-derived CMs

To confirm the identity of hPSC-derived cells, we evaluated the expression of cardiac-specific transcription factors and structural genes at each stage of differentiation. Expression of Nkx2.5, the crucial cardiac transcription factor, was observed throughout the differentiation period in both hESC- (Fig. 2A a, b, and d) and hiPSC-derived CMs (Fig. 2A f, g, and i). The cardiac specific protein, cardiac troponin (Tn) I, which regulates the contraction of cardiac cells, was also expressed in both hESC- and hiPSC-derived CMs at day 12 (Fig. 2A a and f); however, expression was higher in hESC-derived CMs (Fig. 2A a). The cardiac structural gene, αMHC, was expressed in day 18 cells (Fig. 2A b and g), and ANF, an endocrine factor secreted by immature cardiomyocytes, was highly expressed in hPSC-derived CMs at day 24 (Fig. 2A d and i). To confirm the expression of specific markers in single CMs, each stage CMs were replated and cultured. Nuclear NKx2.5 (green) and cytoplasmic αMHC and ANF (red) expressions were observed in replated CMs. (Fig. 2A c, e, h, and j).

Gene expression was evaluated by quantitative reverse transcription PCR (qRT-PCR). Differentiated cells from both hESCs and hiPSCs expressed the cardiac transcription factors Nkx2.5 and Tbx5 (Fig. 2B), and the expression levels were highest in day 18 hESC-derived CMs. Expression of αMHC decreased as differentiation progressed. Unlike hESC-derived CMs, hiPSC-derived CMs expressed cardiac specific genes, but their expression did not increase as dramatically as they did in hESC-derived CMs.

Fig. 3 Aging phenomenon in hPSC-derived CMs. Various assays were used for the evaluation of aging-related phenomena. **A** SA-β-gal staining was performed in each stage of hPSC-derived CMs. Beta-gal-stained cells were observed under the microscope, and small (40× magnification, *inset*) and enlarged images (100× magnification) are represented: *a–d* hESC-derived CMs; *e–h* hiPSC-derived CMs. *a, e* Beta-gal-stained CMs in a whole plate; *b, f* stage 1 (day 12); *c, g* stage 2 (day 18); *d, h* stage 3 (day 24); *i* the number of SA-β-gal-stained cells was counted under a microscope. As indicated by the drawn *bars*, the number of positively stained cells increased as in vitro differentiation progressed and this number increased significantly through stage 2 (day 18) and stage 3 (day 24). **B** Ultrastructural analysis of aged CMs using transmission electron microscopy. Observation of lipofuscin, an aging pigment, within aged cells at each stage was performed. The *yellow asterisk* indicates the prescence of pigment. *a* hESC-derived CM at day 18 (stage 2) showed faint precipitation of aging pigment; *b* hESC-derived CM at day 24 (stage 3) showed accumulated lipofuscin pigment spots; *c* hiPSC-derived CM at day 18 (stage 2) showed relatively abundant small spots of lipofuscin; *d* hiPSC-derived CM at day 24 (stage 3) showed larger, accumulated lipofuscin pigmentation. **C** Expression of aging-related genes in hPSC-derived CMs measured by qRT-PCR. The expression of hTR, a gene encoding the RNA components of telomerase, decreased in days 18 and 24 hESC-derived CMs. The expression of TRF2 also decreased in days 18 and 24 CMs. The expression pattern of hTR and TRF2 in hiPSC-derived CMs differed from hESC-derived CMs, as they did not demonstrate significantly decreased expression in stages 2 and 3. **D** Expression of cell cycle-related genes in hPSC-derived CMs measured by qRT-PCR. The expression of cyclin D1, cyclin D2, cyclin D3, and Cdk2 decreased with each progressing stage of differentiation. The expression of cyclin D3 and Cdk2 decreased as differentiation proceeded in both CMs
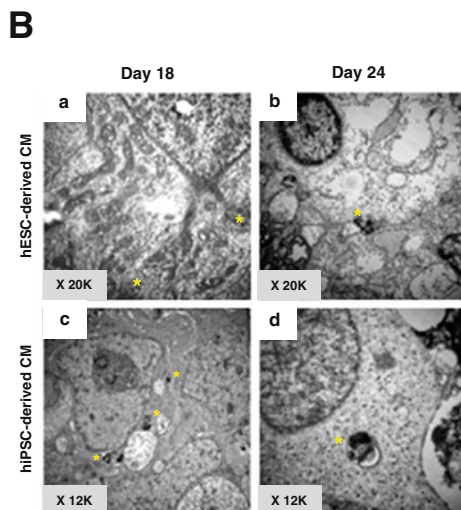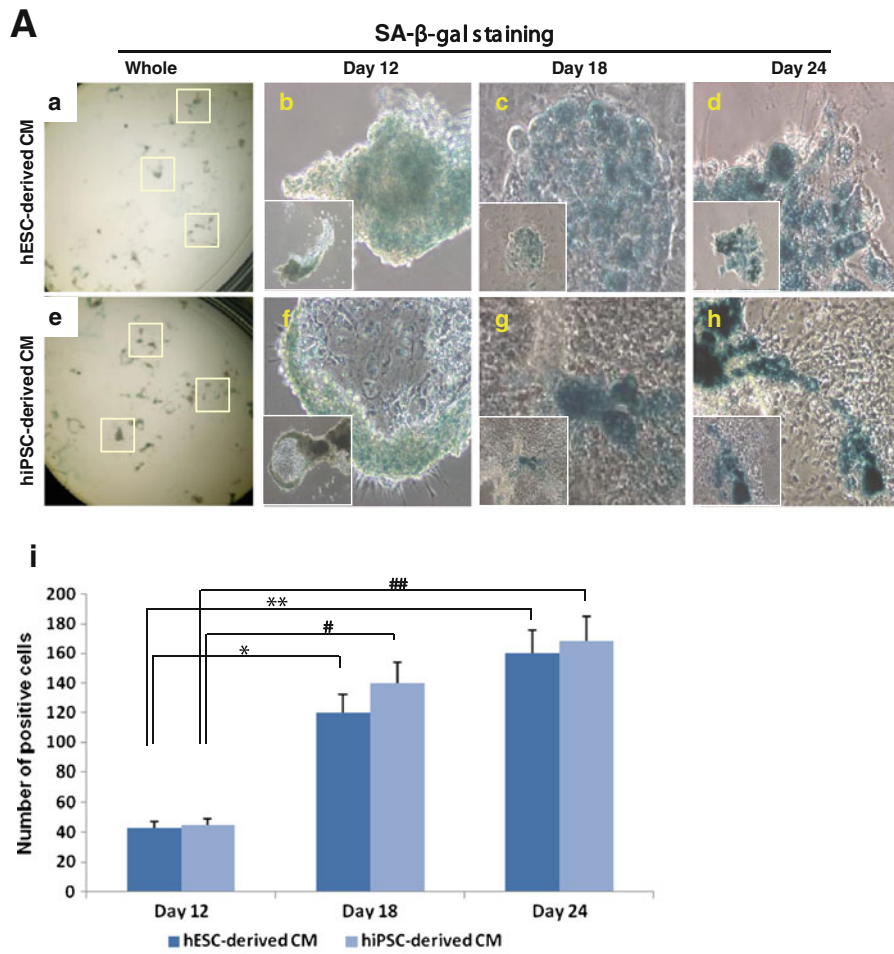
FACS analysis measured the homogeneity of differentiated cell population. In day 24 hESC-derived CMs, the Nkx2.5-positive population comprised 60.5 % of the cells and αMHC-positive cells accounted for 43.7 % (Fig. 2C). Cardiac marker-positive cells in hiPSC-derived CMs accounted for
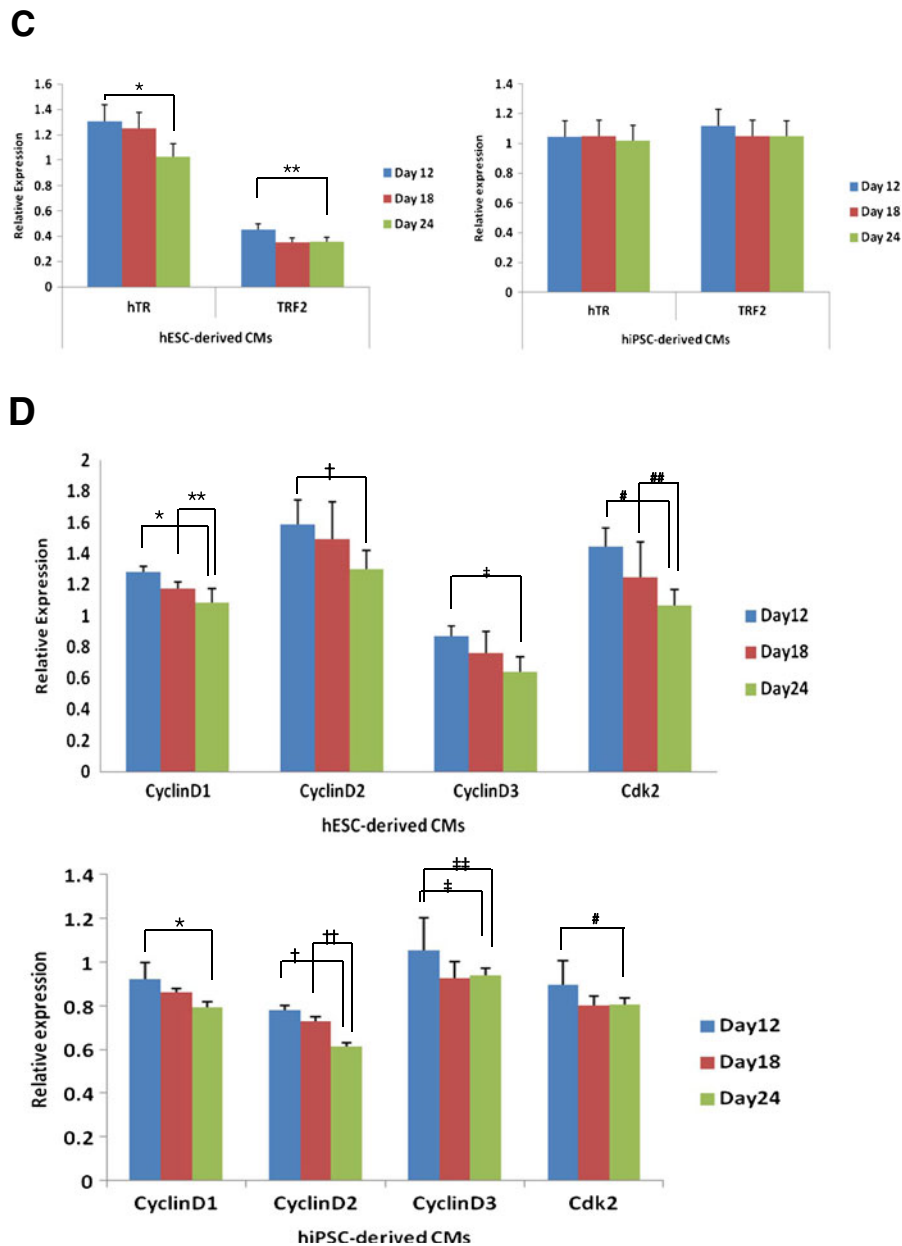
C

D

Fig. 3 (continued)

50 % of the population (data not shown). We isolated and replated the homogeneous region of differentiated cells and processed them for further analysis.

These results demonstrate that differentiated cells from hPSCs possess cardiac characteristics, and prove that the differentiation method previously described by our group can be widely applied for the generation of cardiomyocytes using various hPSC lines.

Aging phenomenon in hPSC-derived CMs

To eliminate the suboptimal condition that may influence the aging process, we confirmed that the medium pH value was ranged from 7.23 to 7.41 throughout all culture stages regardless of adding vitamin C. Differentiated hPSC-derived CMs demonstrated a darkened non-transparent morphology (Fig. 1b). To assess and quantify the aging phenomenon, we performed the

senescence-associated beta-galactosidase (SA-β-gal) assay for each stage of differentiation (Fig. 3A a and e). As shown in Fig. 3A, both hPSC-derived cells were positively stained. Day 12 cells were lightly stained with β-gal in both hPSC-derived CMs (Fig. 3A b and f). Day 24 differentiated cells (Fig. 3A d and h) were strongly stained compared to days 12 and 18 cells (Fig. 3A c and g). The number of β-gal-stained cells increased in correlation to the days of differentiation for both hESC- and hiPSC-derived CMs (Fig. 3A i).

The well-known aging-related pigment lipofuscin was observed in hESC- and hiPSC-derived CMs (Fig. 3B a–d). Lipofuscin was hardly observed in day 18 hESC-derived CMs; however, in day 24 hESC-derived CM, accumulated lipofuscin was clearly observed (Fig. 3B b). In hiPSC-derived CMs, lipofuscin was observed at an earlier stage (day 18, Fig. 3B c) than hESC-derived CMs (Fig. 3B a) and was more pronounced in day 24 CMs (Fig. 3B d). These results demonstrated the time-dependent accumulation of aging-marker pigment in hPSC-derived CMs and its relatively earlier accumulation in hiPSC-derived CMs.

The expression of aging-related genes hTR and TRF2 was evaluated (Fig. 3C). hTR, which encodes the RNA components of telomerase, showed decreased expression in hESC-derived CMs. However, the expression of hTR in hiPSC-derived CMs did not significantly decrease in culture. Another important factor of senescence, TRF2, which is responsible for the protection of human telomeres, demonstrated downregulation in aged hESC-derived CMs; however, no significant difference was observed between stages of differentiation in hiPSC-derived CMs.

Aging of hPSC-derived CMs was accompanied with downregulation of cell cycle-related genes. The expressions of cyclin D1, cyclin D2, cyclin D3, and Cdk2 decreased in hESC- and hiPSC-derived CMs with each successive stage (Fig. 3D).

Anti-aging effects of vitamin C on hESC-derived CMs

Since the natural aging phenomenon was observed more clearly in hESC-derived CMs, these cells served as our model for further studies. We added the well-known anti-aging factor vitamin C to evaluate its effects on aging. To evaluate its effects, vitamin C was added at 0, 100, and 250 μM to days 12, 18, and 24 hESC-derived CMs. Vitamin C treatment at 100 μM proved to be the most effective concentration, and the most

effective duration of treatment was 48 h. Vitamin C-treated CMs (Fig. 4A c and d) showed relatively lower intensity in SA-β-gal staining when compared to non-treated cells (CTL) (Fig. 4A a and b). The effect of vitamin C was also confirmed in days 18 and 24 hESC-derived CMs as the amount of SA-β-gal-positive staining also decreased in these cells (Fig. 4A e).

We also analyzed vitamin C's effects on telomerase activity and telomerase-related gene expression. Telomerase activity was reversed in the vitamin C-treated group, and this result was more apparent in later-stage differentiated cells (Fig. 4B a). We also evaluated the expression of hTR, hTERT, and TRF2 (Fig. 4B b). In day 12 cells, expression of hTR did not significantly increase after vitamin C treatment; however, expression did increase in days 18 and 24 hESC-derived CMs. Expression of hTERT and TRF2 was also upregulated in hESC-derived CMs at three different stages. These results indicate that the effect of vitamin C was more apparent in aged cells and was in vitro culture period dependent.

Alterations of functionality in hESC-derived CMs and effects of vitamin C

To assess the functionality of hESC-derived CMs and their alterations during aging, we stained the cells with the mitochondrial membrane potential-specific dye JC-1. The color of JC-1 usually shifts from red to green according to reduced mitochondrial membrane potential. We monitored the fluorescence of hESC-derived CMs for this chromatic change (Fig. 5A). The green- to red-positive cell population correlated to our microscopy results. At day 24, hESC-derived CMs showed reduced membrane potential as indicated by green fluorescence (Fig. 5A a), and their membrane potential increased in the vitamin C-treated group as evidenced by increased red staining. This change in membrane potential was significant in the 100 μM, 48 h-treated group (Fig. 5A c), when compared to the 100 μM, 24 h-treated group (Fig. 5A b). Treatment of vitamin C enhanced red fluorescence, as the percentage of red-positive cells in the treated group ranged from 30 to 40 % (Fig. 5B b and c), a significantly higher proportion in comparison to non-treated cells (Fig. 5B a).

The beating pattern of hESC-derived CMs was also affected by vitamin C. Generally, in culture, hESC-derived CMs show a decrease in beats per minute (bpm) as they age. Treatment with vitamin C increased the bpm of hESC-derived CMs (Fig. 5C). Also, the

Fig. 4 The anti-aging effect of vitamin C on hESC-derived CMs. To reverse the aging phenomenon of hESC-derived CMs, vitamin C at 100 and 250 μM was added for 24 and 48 h. **A** SA-β-gal staining of day 24 hESC-derived CMs after treatment of vitamin C (100 μM). The number of SA-β-gal-stained cells and the intensity of staining were both significantly reduced. *a, b* β-gal-stained, hESC-derived CMs (150× magnification); *c, d* β-gal-stained, hESC-derived CMs following 24 h vitamin C treatment (150× magnification); *e* according to FACS measurement, the number of stained cells significantly decreased after vitamin C treatment. **B** Telomerase activity and expression of telomere-related genes hTR and hTERT at each stage of hESC-derived CM differentiation. *a* Telomerase activity in hESC-derived CMs. The product of each group was sequentially loaded. The *left lane* holds non-treated control and the *right lane* holds the respective vitamin C 100 μM 48 h-treated groups. *b* Expressions of telomerase-related genes, hTR and hTERT, and TRF2 were analyzed for each stage in hESC-derived CMs. Gene expression between the control group and vitamin C-treated group is compared
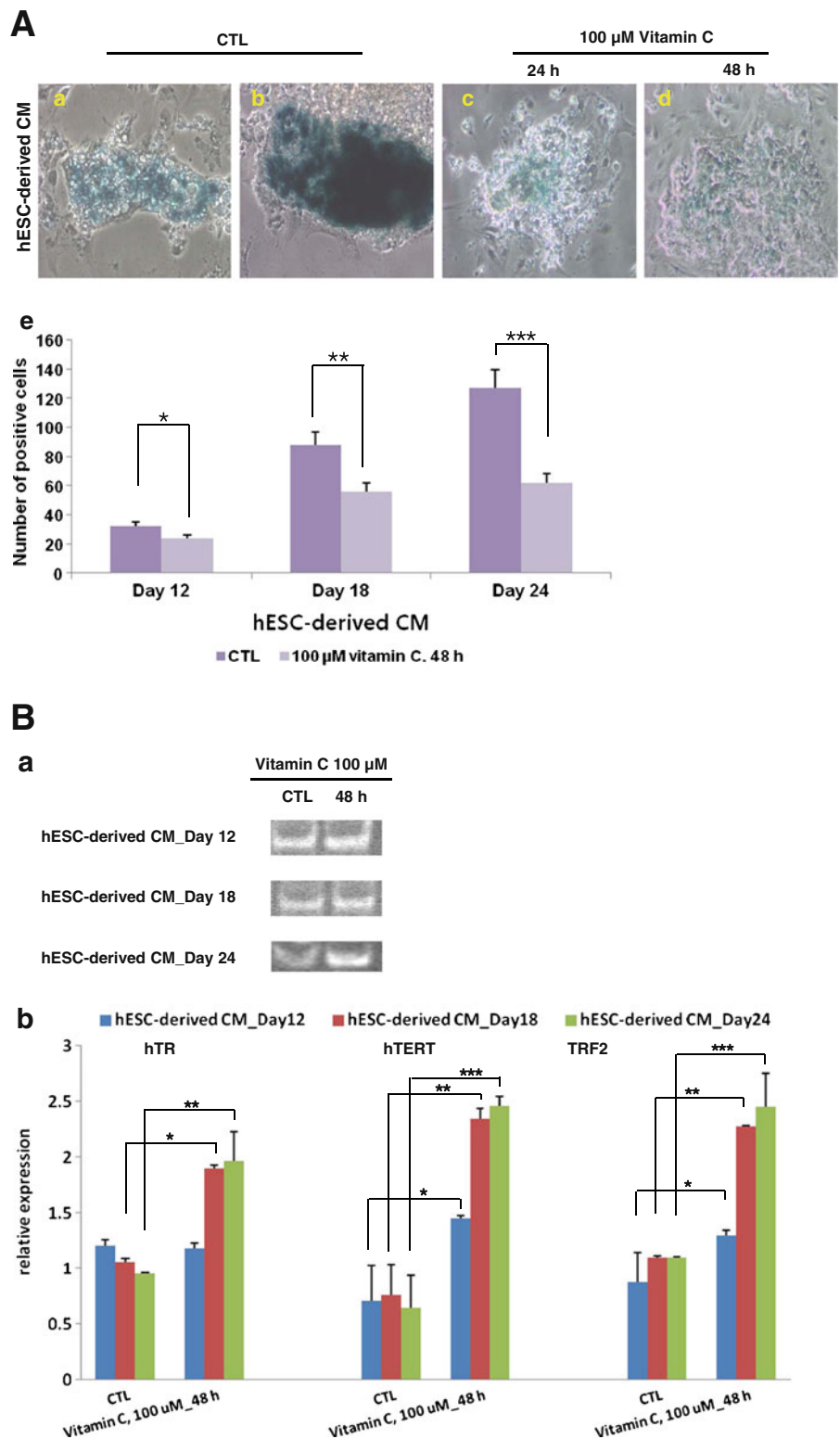
Fig. 5 Alterations of functionality in hESC-derived CMs. The addition of vitamin C enhanced the mitochondrial function and beating frequency of hESC-derived aged CMs. **A** JC-1, which exhibits potential-dependent accumulation in mitochondria, was used as an indicator of mitochondrial potential. Vitamin C treatment significantly enhanced JC-1 red fluorescence (polarization, high membrane potential). Conversely, JC-1 green fluorescence (depolarization, low membrane potential) was reduced in hESC-derived CMs at day 24 when treated with vitamin C. *a* Control; *b* vitamin C 100 μM, 24 h; *c* vitamin C 100 μM, 48 h. **B** Population of JC-1 positive cells. JC-1 stained, hESC-derived CMs at day 24 were dissociated into single cells then immediately analyzed using flow cytometry. The red fluorescence-positive population increased when treated with vitamin C. *a* Control; *b* vitamin C 100 μM, 24 h; *c* vitamin C 100 μM, 48 h. **C** Effect of vitamin C on beating frequency of hESC-derived CMs. Treated CMs showed a smaller reduction in beating frequency compared to control
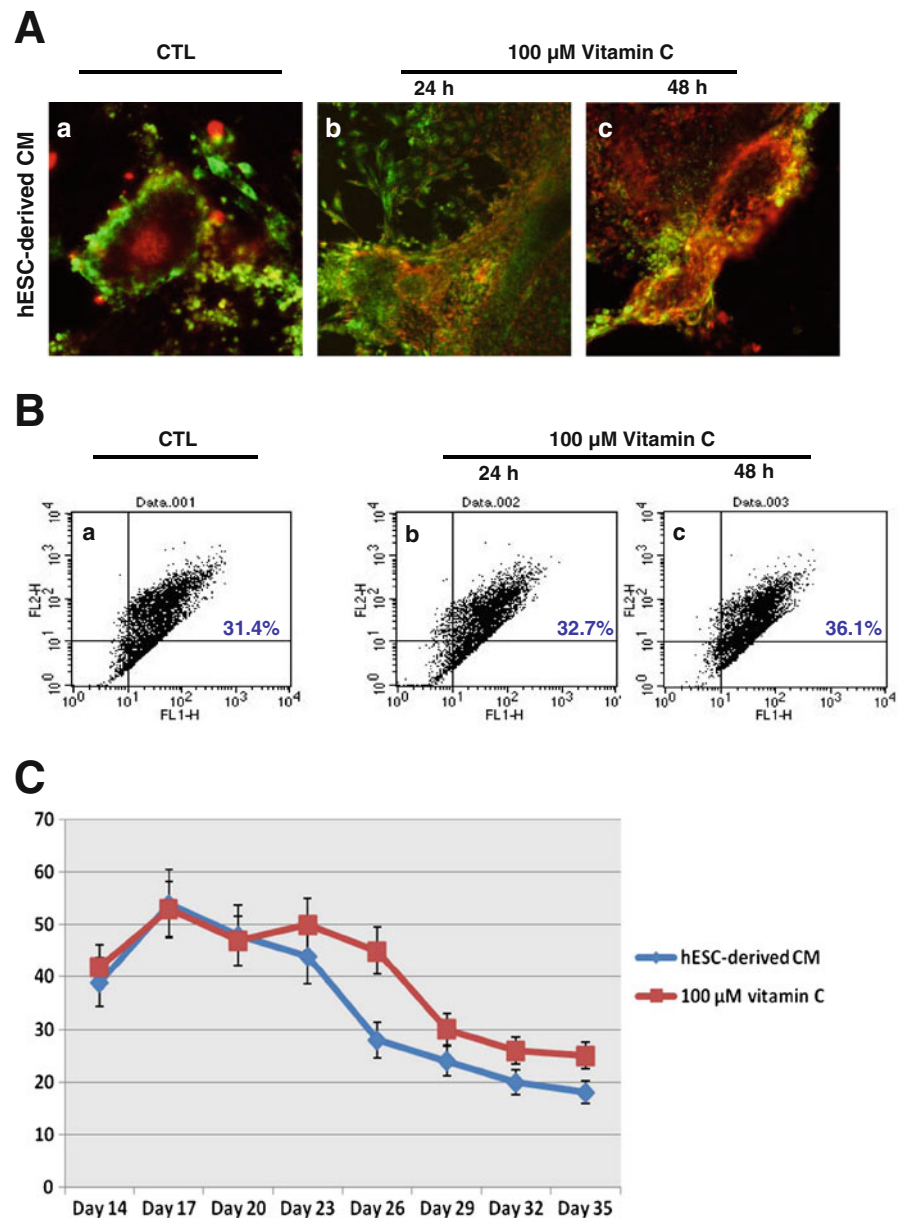
duration of beating was longer in CMs treated with vitamin C.

Discussion

Biomedical research seeks explanations for the phenomena of human metabolism and its mechanisms. This research needs human cells from the body's various organ systems; however, for clinical and ethical reasons, live tissues from the human body itself cannot be practically acquired to serve as a basic biomedical research model. hESCs derived from the inner cell mass of embryo (Thomson et al. 1998) and hiPSCs derived from a patient's fibroblasts (Takahashi et al. 2007) can serve as suitable alternatives for human studies due to their

origins and developmental potential (Pera et al. 2000; Reubinoff et al. 2000). Human stem cell derivatives such as cardiac cells are a unique and reproducible cellular model for use in human developmental biology, biomedical research, and pharmaceutical studies.

Aging is the general phenomenon that affects somatic cells and leads to decreased cellular and body function, represented by the shortening of telomeres, the accumulation of mutations, and the development of mitochondrial dysfunction (Goldstein 1990; Finkel and Holbrook 2000). The aging phenomenon is temporally extensive; therefore, research on the aging of the human body cells is difficult to conduct. Aging of cardiomyocytes is caused by age, reactive oxidative species formation, and mitochondrial damage (Terman et al. 2004; Terman and Brunk 2005). These effects are reproducible in in vitro culture of cardiomyocytes.

Here, we demonstrated the aging phenomenon in hPSC-derived CMs. Human PSC-derived CMs spontaneously aged in in vitro culture conditions. Day 24 cells showed a more age-specific pigmented appearance than cells at days 12 and 18. These morphological changes correlated with decreased expression of cell cycle-related genes, slower beating rates, and lower mitochondrial membrane potentials. The expression of cyclin genes decreased in a time-dependent manner. This downregulation of cyclin genes in our study was similar to known general changes in aging at the molecular level (Sheydina et al. 2011). Our finding of slower beating in aged cells was consistent with our previous report (Kim et al. 2011). We measured mitochondrial functionality using JC-1 dye at day 24 and found that only 30 % of differentiated cells preserved mitochondrial function. Additionally, the expression of telomere encoding genes was downregulated.

An interesting finding is that less prominent feature of aging and of vitamin C's reverse effects was observed in hiPSC-derived CM. Human iPSCs are adult somatic cells that have been reprogrammed to a pluripotent state (Yu et al. 2007) through delivery of exogenous pluripotency factors (Takahashi et al. 2007). Due to the nature of their derivation, iPSCs are considered to possess a different epigenetic state from ESCs (Chin et al. 2009) and also demonstrate reduced differentiation efficiency into specific lineages (Mauritz et al. 2008). The exogenous reprogramming factors chosen for insertion into somatic cells may account for this finding. Reprogrammed hiPSCs have shown incomplete reprogramming or early senescence

during in vitro differentiation when compared to hESCs (Hanna et al. 2010). Thus, hESC-derived CMs seem to be more suitable for the study of aging or related research.

Vitamin C has many roles in anti-aging and has shown cardiovascular-protective effects (Zhou et al. 2006; Luiking et al. 2010). We used various concentration of vitamin C to demonstrate these anti-aging effects on hESC-derived CMs. Vitamin C treatment affected the beating frequency of hESC-derived CMs and alleviated the tendency hESC-derived CMs have of beating more slowly with age. Furthermore, treatment with vitamin C affected the expression of aging-related genes and mitochondrial function in hESC-derived CMs. Firstly, changes in hTERT, hTR, and TRF2 were observed. Human TR (hTR) and hTERT encode human telomerase-related RNA and protein, respectively. Their role in aging is well known (Hiyama et al. 1995) as both genes are related to telomeres and telomerase (Huffman et al. 2000; Blackburn 2001). In our study, treatment with vitamin C in different staged CMs increased the expression of hTERT. Human TR expression also increased in late-stage hESC-derived CMs. These results demonstrate that vitamin C has direct effects on telomerase activity in hESC-derived CMs. Furthermore, vitamin C may enhance the transcription of telomerase-related genes, and this anti-aging effect may be stage dependent in aged hESC-derived CMs. Expression of TRF2 dramatically increased in late stage of hESC-derived CMs treated with vitamin C, and these results show that TRF2 plays a role in the genetic regulation of aged hESC-derived CMs. TRF2 activity is linked to aging in somatic cells, which further suggests the anti-aging effects generated by vitamin C.

We also observed the effect of vitamin C on mitochondrial membrane potential. The anti-aging effect of vitamin C correlated with the recovery of beating rate in hESC-derived CMs. Taken together, these results show that the well-known cardioprotective role of vitamin C also applies to hESC-derived CMs in vitro. Among the tested conditions, vitamin C treatment at 100 μM for 48 h was most effective and this concentration is close to the recommended dietary allowance of vitamin C. These results strongly support the validation of hESC-derived CMs as a viable cell source which can serve as a unique model of human heart cell aging.

In conclusion, we have shown that hESC-derived CMs are suitable for use as an alternative model for

aging in human cardiac cells. This model can be extended to other areas of biomedical research as an alternative to primary human heart cells, and various candidate anti-aging factors can thus be studied with hESC-derived CMs in the future.

References

Blackburn EH (2001) Switching and signaling at the telomere. Cell 106:661–673

Chin MH, Mason MJ, Xie W, Volinia S, Singer M, Peterson C, Ambartsumyan G, Aimiuwu O, Richter L, Zhang J, Khvorostov I, Ott V, Grunstein M, Lavon N, Benvenisty N, Croce CM, Clark AT, Baxter T, Pyle AD, Teitell MA, Pelegrini M, Plath K, Lowry WE (2009) Induced pluripotent stem cells and embryonic stem cells are distinguished by gene expression signatures. Cell Stem Cell 5:111–123

Finkel T, Holbrook NJ (2000) Oxidants, oxidative stress and the biology of ageing. Nature 408:239–247

Goldstein S (1990) Replicative senescence: the human fibroblast comes of age. Science 249:1129–1133

Hanna JH, Saha K, Jaenisch R (2010) Pluripotency and cellular reprogramming: facts, hypotheses, unresolved issues. Cell 143:508–525

Hiyama E, Yokoyama T, Tatsumoto N, Hiyama K, Imamura Y, Murakami Y, Kodama T, Piatyszek MA, Shay JW, Matsuura Y (1995) Telomerase activity in gastric cancer. Cancer Res 55:3258–3262

Huffman KE, Levene SD, Tesmer VM, Shay JW, Wright WE (2000) Telomere shortening is proportional to the size of the G-rich telomeric 3′-overhang. J Biol Chem 275:19719–19722

Kehat I, Kenyagin-Karsenti D, Snir M, Segev H, Amit M, Gepstein A, Livne E, Binah O, Itskovitz-Eldor J, Gepstein L (2001) Human embryonic stem cells can differentiate into myocytes with structural and functional properties of cardiomyocytes. J Clin Invest 108:407–414

Kim YY, Ku SY, Jang J, Oh SK, Kim HS, Kim SH, Choi YM, Moon SY (2008) Use of long-term cultured embryoid bodies may enhance cardiomyocyte differentiation by BMP2. Yonsei Med J 49:819–827

Kim YY, Ku SY, Liu HC, Cho HJ, Oh SK, Moon SY, Choi YM (2011) Cryopreservation of human embryonic stem cells derived-cardiomyocytes induced by BMP2 in serum-free condition. Reprod Sci 18:252–260

Laflamme MA, Murry CE (2005) Regenerating the heart. Nat Biotechnol 23:845–856

Luiking YC, Engelen MP, Deutz NE (2010) Regulation of nitric oxide production in health and disease. Curr Opin Clin Nutr Metab Care 13:97–104

Mauritz C, Schwanke K, Reppel M, Neef S, Katsirntaki K, Maier L, Nguemo F, Menke S, Haustein M, Hescheler J, Hasenfuss G, Martin U (2008) Generation of functional murine cardiac myocytes from induced pluripotent stem cells. Circulation 118:507–517

Mummery C, Ward-van Oostwaard D, Doevendans P, Spijker R, van den Brink S, Hassink R, van der Heyden M, Opthof T, Pera M, de la Riviere AB, Passier R, Tertoolen L (2003) Differentiation of human embryonic stem cells to cardiomyocytes: role of coculture with visceral endoderm-like cells. Circulation 107:2733–2740

Oh SK, Kim HS, Ahn HJ, Seol HW, Kim YY, Park YB, Yoon CJ, Kim DW, Kim SH, Moon SY (2005a) Derivation and characterization of new human embryonic stem cell lines: SNUhES1, SNUhES2, and SNUhES3. Stem Cells 23:211–219

Oh SK, Kim HS, Park YB, Seol HW, Kim YY, Cho MS, Ku SY, Choi YM, Kim DW, Moon SY (2005b) Methods for expansion of human embryonic stem cells. Stem Cells 23:605–609

Pera MF, Reubinoff BE, Trounson A (2000) Human embryonic stem cells. J Cell Sci 113:5–10

Reubinoff BE, Pera MF, Fong CY, Trounson A, Bongso A (2000) Embryonic stem cell lines from human blastocysts: somatic differentiation in vitro. Nat Biotechnol 18:399–404

Sheydina A, Riordon DR, Boheler KR (2011) Molecular mechanisms of cardiomyocyte aging. Clin Sci 121:315–329

Takahashi K, Tanabe K, Ohnuki M, Narita M, Ichisaka T, Tomoda K, Yamanaka S (2007) Induction of pluripotent stem cells from adult human fibroblasts by defined factors. Cell 131:861–872

Terman A, Brunk UT (1998) On the degradability and exocytosis of ceroid/lipofuscin in cultured rat cardiac myocytes. Mech Ageing Dev 100:145–156

Terman A, Brunk UT (2005) The aging myocardium: roles of mitochondrial damage and lysosomal degradation. Heart Lung Circ 14:107–114

Terman A, Dalen H, Eaton JW, Neuzil J, Brunk UT (2003) Mitochondrial recycling and aging of cardiac myocytes: the role of autophagocytosis. Exp Gerontol 38:863–876

Terman A, Dalen H, Eaton JW, Neuzil J, Brunk UT (2004) Aging of cardiac myocytes in culture: oxidative stress, lipofuscin accumulation, and mitochondrial turnover. Ann N Y Acad Sci 1019:70–77

Thomson JA, Itskovitz-Eldor J, Shapiro SS, Waknitz MA, Swiergiel JJ, Marshall VS, Jones JM (1998) Embryonic stem cell lines derived from human blastocysts. Science 282:1145–1147

Yokoo N, Baba S, Kaichi S, Niwa A, Mima T, Doi H, Yamanaka S, Nakahata T, Heike T (2009) The effects of cardioactive drugs on cardiomyocytes derived from human induced pluripotent stem cells. Biochem Biophys Res Commun 387:482–488

Yu J, Vodyanik MA, Smuga-Otto K, Antosiewicz-Bourget J, Frane JL, Tian S, Nie J, Jonsdottir GA, Ruotti V, Stewart R, Slukvin II, Thomson JA (2007) Induced pluripotent stem cell lines derived from human somatic cells. Science 318:1917–1920

Zhou H, Ma JH, Zhang PH, Luo AT (2006) Vitamin C pretreatment attenuates hypoxia-induced disturbance of sodium currents in guinea pig ventricular myocytes. J Membr Biol 211:81–87